Journal of Medicinal Chemistry Article

J. Med. Chem. **2010,** *53,* 2087–2093 **2087**
DOI: 10.1021/jm901534d

Structural Basis for Platelet Antiaggregation by Angiotensin II Type 1 Receptor Antagonist Losartan (DuP-753) via Glycoprotein VI

Katsuki Ono,[†,‡] Hiroshi Ueda,[†,§] Yoshitaka Yoshizawa,[†,§] Daisuke Akazawa,[†,§] Ryuji Tanimura,[†,§] Ichio Shimada,*[,‡,∥] and Hideo Takahashi*[,‡]

[†]*Japan Biological Informatics Consortium* (*JBIC*), *Aomi 2-41-6, Koto-ku, Tokyo 135-0064, Japan,*
[‡]*Biomedicinal Information Research Center* (*BIRC*), *National Institute of Advanced Industrial Science and Technology* (*AIST*), *Aomi 2-41-6, Koto-ku, Tokyo 135-0064, Japan,* [§]*Toray Branch Office of JBIC, Tebiro 6-10-1, Kamakura-shi, Kanagawa 248-8555, Japan, and* [∥]*Graduate School of Pharmaceutical Sciences, The University of Tokyo, Hongo 7-3-1, Bunkyo-ku, Tokyo 113-0033, Japan*

Received October 16, 2009

GPVI is a key receptor for collagen-induced platelet activation. Loss or inhibition of GPVI causes only mildly prolonged bleeding times but prevents arterial thrombus formation in animal models. Therefore, GPVI is considered to be a potent target molecule for therapy of thrombotic diseases. Recently, it was reported that the AT_1-receptor antagonist losartan (DuP-753) and EXP3179 inhibit platelet adhesion and aggregation via GPVI. However, it is still not clear how losartan is associated with inhibition of binding between GPVI and collagen at the molecular level. Here, we show by NMR that losartan directly interacts with the hydrophobic region consisting of strands C′ and E in the N-terminal Ig-like domain of GPVI. A reliable GPVI−losartan complex model is presented by using a combination of NMR data and in silico tools. These data indicated that the phenyl group with the tetrazole ring in losartan plays a crucial role in the interaction with GPVI.

Introduction

Platelet adhesion and aggregation to collagen exposed at injured vascular endothelium are fundamental requirements for platelet function. Arterial thrombosis formation underlying acute coronary syndromes (ACS[a]) or stroke occurs by the normal function of platelets.[1] The platelet collagen receptor, glycoprotein (GP) VI, is primarily responsible for regulating initial platelet adhesion and aggregation in flowing blood. GPVI predominantly mediates intracellular signaling that leads to activation of the platelet integrin $\alpha_{IIb}\beta_3$, which binds fibrinogen or vWF and mediates platelet aggregation.[2,3]

The evidence that GPVI is an important molecule for platelet aggregation is as follows: (1) GPVI-deficient platelets have almost no response to collagen stimulation;[4] (2) Fab fragments of an anti-GPVI antibody inhibit collagen-stimulated platelet aggregation;[5] (3) in mice, soluble GPVI-Fc dimers inhibit platelet aggregation to injured vessel walls in vivo.[6] Therefore, GPVI is considered to be a target protein for therapeutic drug design in arterial thrombotic diseases (e.g., ACS and stroke). Losartan (DuP-753) is a prodrug that is actively metabolized by the cytochrome P450 isoenzyme CYP2C9 on first liver passage,[7] and its main antihypertensive AT_1-receptor blocking metabolite, 2-butyl-4-chloro-1{[2′-(1*H*-tetrazol-5-yl)[1,1′-biphenyl]-4-yl]methyl}-1*H*-imidazole-5-carboxylic acid (EXP3174),[8] is 10- to 40-fold more potent than the prodrug form. 2-Butyl-4-chloro-1{[2′-(1*H*-tetrazol-5-yl)[1,1′-biphenyl]-4-yl]methyl}-1*H*-imidazole-5-carboxaldehyde (EXP3179)[8] was originally identified as an aldehyde metabolite of losartan in patients after administration and is also produced as a hepatic metabolite by the cytochrome P450 pathway. Since the early 1990s, AT_1-receptor antagonists like losartan have made up a new generation of antihypertensive agents that also modulate hemostasis, and apparently this effect is not solely the result of AT_1-receptor blockage. AT_1-receptor antagonists are potent in releasing nitric oxide (NO) in a concentration-dependent manner for platelet and endothelial cells.[9] It has been indicated that NO, a potent inhibitor of platelet adhesion and aggregation, directly inhibits TXA_2-dependent platelet activation.[10] Among the tested AT_1-receptor antagonists, the inhibitory effect of losartan on platelet adhesion and aggregation is higher those that of **1** (EXP3174) and valsartan[9] and is not shared by candesartan.[11]

Sole administration of the NO synthase (NOS) inhibitor L-NAME does not change collagen-stimulated adhesion and aggregation, but NOS inhibition markedly attenuates antiadhesion and antiaggregation effects of losartan.[9] In this regard, the application of losartan itself impairs collagen-induced platelet adhesion and aggregation. Grothusen et al. recently reported that losartan and **2** (EXP3179) function as specific inhibitors of the platelet collagen receptor GPVI independent of AT_1-receptor antagonism.[12] This result indicates that GPVI activating antibody 4C9 prevents the inhibitory effect of platelet aggregation that depends on the losartan and **2** dose. However, there is no evidence that losartan and **2**

*To whom correspondence should be addressed. For I.S.: (address) Graduate School of Pharmaceutical Sciences, The University of Tokyo, Hongo 7-3-1, Bunkyo-ku, Tokyo 113-0033, Japan; (phone/fax) +81-3-3815-6540; (e-mail) shimada@iw-nmr.f.u-tokyo.ac.jp. For H.T.: (phone) +81-3-3599-8090; (fax) +81-3-3599-8099; (e-mail) hid.takahashi@aist.go.jp.

[a] Abbreviations: GPVI, glycoprotein VI; AT_1, angiotensin II type 1; ACS, acute coronary syndrome; vWF, von Willebrand factor; TXA_2, thromboxane A_2; NOS, nitric oxide synthase; L-NAME, N^G-nitro-L-arginine methyl ester; CRP, collagen-related peptide; CSP, chemical shift perturbation; IFD, induced fit docking.

Published on Web 02/16/2010

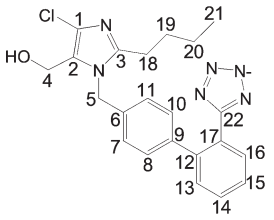

Figure 1. Chemical structure of losartan. Aliphatic groups, aromatic protons, and the methyl group are labeled with numbers. Only the carbon atoms are labeled in the figure.

inhibit platelet adhesion and aggregation for binding to GPVI at the molecular level.

In this work, we analyzed in detail the interaction of GPVI with losartan by a combination of NMR spectroscopy and in silico tools. We show that losartan directly interacts with the N-terminal Ig-like domain ($D1^{GPVI}$, 1−91 aa) of GPVI consisting of strands C′ and E by using a chemical shift perturbation (CSP) experiment. We produced possible orientations of losartan against the ligand binding site determined by CSP by using in silico tools. The ligand docking poses on the GPVI surface were grouped according to both the docking score of each program and rmsd cluster analysis. To generate a more reliable protein−ligand complex structure, candidate GPVI−losartan complex models were selected using intermolecular NOEs. Finally, selected models were tested for stability by molecular dynamics (MD) simulations. MD simulations and other experimental data indicated that the phenyl group with the tetrazole ring in losartan is the key chemical structure for interaction with GPVI.

Results

Evaluation of $D1D2^{GPVI}$ Purified from *E. coli*. To investigate if the recombinant GPVI Ig-like domain ($D1D2^{GPVI}$, 1−184 aa), which was purified and refolded from inclusion bodies, interacts with its ligands, kinetic analyses were performed by using SPR. Reportedly, GPVI recognizes the Gly-Pro-Hyp (GPO; Hyp is hydroxyproline) motif in the triple helical structure of collagen.[13,14] The collagen-related peptide (CRP), which contains 10 GPO motifs, is a specific agonist for GPVI. Furthermore, GPVI specifically recognizes CRP and human collagen type I and type III but not a peptide of similar sequence, Gly-Pro-Pro (GPP), that lacks hydroxyproline.[15] Therefore, we used CRP and human collagen type I as ligands of GPVI for evaluation of $D1D2^{GPVI}$ kinetic activity in collagen binding. CRP and collagen type I were immobilized on sensor chips at low pH, and the interactions between flowing $D1D2^{GPVI}$ and immobilized ligands were measured under physiological conditions. Sensorgrams for several analyte concentrations were obtained and normalized by subtracting the background responses from collagen type I and CRP (Figure 2). Dissociation constants (K_D) of $D1D2^{GPVI}$ against collagen type I or CRP were obtained by using the steady-state affinity analysis method in BIAeval 4.1 (BIAcore AB). The K_D values of $D1D2^{GPVI}$ against collagen and CRP were 1.8×10^{-4} and 1.3×10^{-5} M, respectively. This K_D of $D1D2^{GPVI}$ against CRP is virtually the same as that of the GPVI extracellular domain, which is expressed in human cells.[16]

NMR Resonance Assignments of $D1D2^{GPVI}$. Backbone assignments of $D1D2^{GPVI}$ were established by using two- and three-dimensional heteronuclear NMR spectroscopy. Initial NMR sample preparations of $D1D2^{GPVI}$ suggested partial aggregation of the protein, as evident by a relatively low spectral signal-to-noise ratio and considerable variation of cross-peak intensity in the 2D $^1H-^{15}N$ HSQC spectrum. Optimization of the NMR sample conditions, including data collection at elevated temperatures up to 310 K and addition of glycerol, significantly improved the quality of the NMR spectrum. Under optimized conditions, we performed 3D NMR measurements of $D1D2^{GPVI}$ at 200 μM protein concentration. In order to confirm the resonance assignment, we measured the 2D TROSY-HN(CO) spectra of $^2H,^{15}N$-labeled samples with 1-^{13}C amino acid selective labeling.[17] As a result, 78.7% of the backbone amide resonances (excluding 20 proline residues) of $D1D2^{GPVI}$ were assigned. The assignment is nearly complete for $D1^{GPVI}$ (92.6%), while only 65.1% of the resonances originating from $D2^{GPVI}$ (C-terminal Ig-like domain, 92−184 aa) could be assigned. The residues that could not be assigned in $D2^{GPVI}$ were not scattered over a large region but rather located in local regions such as strands B, C, C′, and E in $D2^{GPVI}$. Considering the fact that these regions have a higher *B* factor than other regions in $D2^{GPVI}$ in the crystal structure,[18] there may be minor conformations or slow exchange dynamics in these regions.

Interaction Analysis between GPVI and Losartan. Grothusen et al. demonstrated that the inhibition of platelet aggregation by losartan or **2** is prevented by additional stimulation with collagen type I or the selective GPVI-receptor activating antibody 4C9 in human PRP (platelet-rich plasma).[12] Therefore, it is recognized that losartan and **2** inhibit collagen-dependent platelet activation via GPVI. However, there is no evidence of a direct interaction between $D1D2^{GPVI}$ and losartan or **2**. In this study, we first examined the possibility of an interaction between GPVI and losartan by NMR spectroscopy. Losartan inhibits collagen-stimulated platelet aggregation as well as **2**[12] and dissolves more easily at high concentrations. In order to investigate the interaction between GPVI and losartan, 2D $^1H-^{15}N$ TROSY-HSQC spectra of $D1D2^{GPVI}$ were recorded by successive addition of losartan. Some of the cross-peaks in the TROSY-HSQC spectra experienced gradual chemical shift changes upon increasing concentrations of losartan, which suggests that the free and bound states in $D1D2^{GPVI}$ undergo fast exchange on the chemical shift time scale (Figure 3A). None of the cross-peaks of GPVI amide protons exhibited further chemical shift changes at molar ratios beyond 1:12. To identify the losartan recognition site in GPVI, CSP upon binding to losartan was calculated as described in Experimental Section and plotted as a function of the residue number in GPVI (Figure 3B). We observed only nine cross-peaks deviating more than 1.0 ppm at $\Delta\delta$, chemical shift changes between the free and bound states of GPVI, including Glu40-Lys41 located in strand C, Tyr47-Asp49 in strand C′, Phe54-Ile55 in strand E, Met58 in the E-3_{10} loop, and Leu62 in the 3_{10} helix (Figure 3C). Interestingly, the GPVI surface, which is formed by strand C′, strand E, and the 3_{10} helix, contains the hydrophobic putative collagen binding region.[18] We estimated the K_D of losartan with curve fitting using the quadratic equation of chemical shift change as a function of ligand concentration. The K_D of $D1D2^{GPVI}$ and losartan is 1.7×10^{-4} M, indicating that losartan has the same binding affinity for GPVI as human collagen type I.

CSP-Guided Docking Simulation. We obtained 11 and 74 docking poses using rigid and induced fit docking (IFD) protocols in Glide, respectively. We then obtained a total of 38 docking poses after excluding complex models with a

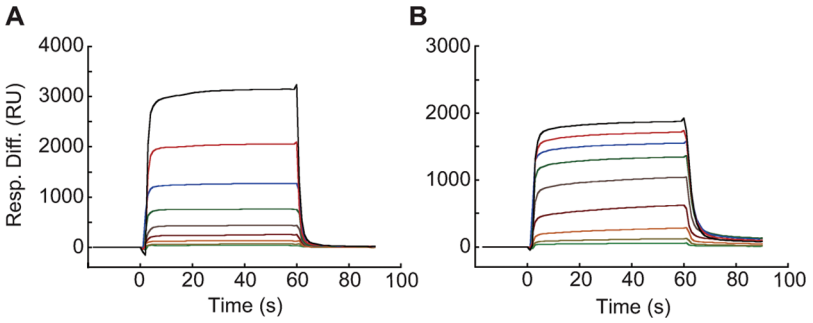

Figure 2. Sensorgrams of the interaction of D1D2^{GPVI} with immobilized ligands. D1D2^{GPVI} solutions flowed over immobilized (a) collagen type I (2700 RU) and (b) CRP-XL (3000 RU) and control surfaces. Each line is colored as follows: black, 200 μM; red, 100 μM; blue, 50 μM; dark-green, 25 μM; sepia, 12.5 μM; wine-red, 6.25 μM; brown, 3.13 μM; olive, 1.56 μM; green, 0.78 μM. Responses from immobilized ligands were subtracted from that of the control surface.

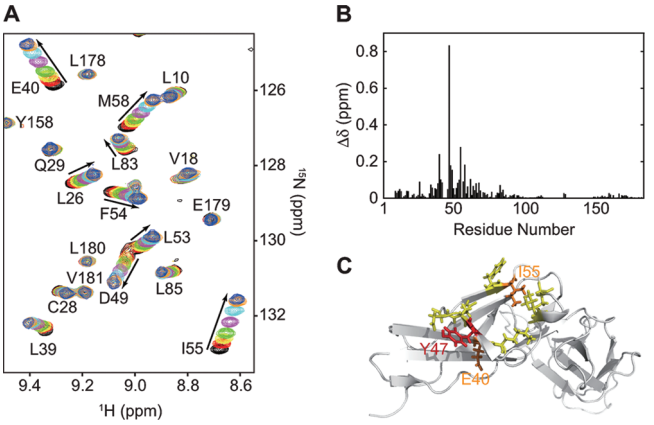

Figure 3. (A) Overlay of expanded region of $^{1}H-^{15}N$ TROSY-HSQC spectra of D1D2^{GPVI} titrated with losartan. Chemical shifts in D1D2^{GPVI} were changed by increasing amounts of losartan from 0 to 1.2 mM as displayed: black, red, yellow, green, magenta, cyan, orange, and blue for 0, 30, 60, 100, 200, 400, and 800 μM and 1.2 mM losartan, respectively. Cross-peaks are labeled with their corresponding residue numbers and a single-letter code. The arrows indicate the direction of chemical shift change during titration of losartan into D1D2^{GPVI}. This figure was generated by using the software SPARKY.[38] (B) Plot of D1D2^{GPVI} chemical shift changes ($\Delta\delta$) between the absence and presence of losartan (1.2 mM) against residue number. $\Delta\delta$ was calculated by using the formula $\Delta\delta = [(\Delta\delta_H)^2 + (\Delta\delta_N/5)^2]^{1/2}$, where $\Delta\delta_H$ and $\Delta\delta_N$ denote chemical shift changes of hydrogen and nitrogen, respectively. (C) CSP data mapped onto the crystal structure of D1D2^{GPVI}.[18] Residues are colored according to the following color scheme: red, $\Delta\delta > 0.4$ ppm; orange, $0.2 < \Delta\delta \leq 0.4$ ppm; yellow, $0.1 < \Delta\delta \leq 0.2$ ppm.

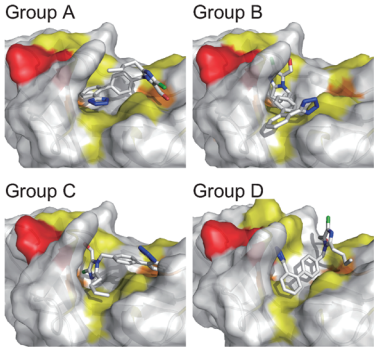

Figure 4. Four representative in silico docking poses of losartan from each group divided by cluster analysis and the binding site of losartan in the GPVI hydrophobic pocket. D1D2^{GPVI} is colored by CSP results (see Figure 3C). Losartan, which is rendered as a stick model, is colored white, blue, red, and green for carbon, nitrogen, oxygen, and chloride, respectively.

more than −6.0 GlideScore (Table S1 in Supporting Information). In Sievgene, we obtained 100 docking poses and selected 25 by excluding complex models with a more than −4.0 Sievgene score (Table S1). Subsequently, we selected one docking pose that had the best score among all of the poses in Glide as the first representative pose. The rmsd values with respect to the best score pose were calculated for all other docking poses. If the rmsd value was lower than 3 Å, then it was grouped into the first cluster. Otherwise, it was identified as the new representative pose in the new cluster. This procedure was repeated while calculating rmsd values with respect to representative poses one by one. On the basis of the rmsd values, all docking poses were classified into 17 distinct poses. These poses were further classified into four groups according to which portion of losartan contacted with the binding pocket of GPVI. In group A, the phenyl group with the tetrazole ring is deeply buried in the pocket. In group B, the alkyl chain is in the binding pocket. In group C, the hydroxymethyl group and chlorine modified imidazole group exist in the pocket. Finally, group D consists of poses in which losartan has no contact with the hydrophobic pocket (Figure 4).

Selection of Ligand Docking Poses by Intermolecular NOE. Intermolecular NOEs were identified by comparisons of 3D ^{15}N-edited NOESY-HSQC spectra between the free and bound states of GPVI. NOESY measurement was performed with 8-fold excess of losartan. As a result, possible intermolecular NOE peaks were found for the amide protons of Lys41 and Gln48 of GPVI (data not shown). These residues were located in the losartan binding region of GPVI determined by the CSP experiments (Figures 3C and 5). To confirm that the intermolecular NOEs originated from losartan, we carried out high resolution 2D ^{15}N(F2)-edited $^{1}H-^{1}H$ NOESY experiments with or without ^{15}N decoupling during an evolution period (data not shown). Comparison of the 1D ^{1}H spectrum of losartan with the high resolution NOESY spectrum (Figure 5) revealed that the amide protons of Lys41 and Gln48 were located in proximity to H15/H16 and H14/H15 of losartan protons (Figure 1), respectively. Among the docking poses, only the docking pose of group A fulfilled all of the intermolecular NOE distance conditions.

Molecular Dynamics Simulation of the GPVI−Losartan Complex. To confirm whether the reliable ligand docking pose in group A is a stable complex structure, we performed MD simulations of the GPVI−losartan complex structure

with explicit water molecules to mimic physiological conditions. $D2^{GPVI}$, which was not affected by the CSP experiment, was omitted from MD simulations to reduce computational complexity. Moreover, the $D1^{GPVI}$ and losartan complex structure had acceptable rotation at the center of gravity and limited translation in explicit water molecules for 5 ns of simulation time.

The motion of losartan in MD simulations was monitored with essential rmsd analysis, compared to the initial losartan structure, and was performed on each chemical structure of losartan (Figure 6A). As a result, the phenyl group with the tetrazole ring of losartan is restricted compared with other chemical structures on the GPVI surface, and furthermore, the imidazole group and alkyl chain had some degree of mobility during 5 ns of simulation. When snapshots of the trajectory were superimposed on the GPVI backbone, the phenyl group and tetrazole ring were restricted in mobility on the GPVI surface (Figure 6B and Figure S1). The MD simulation results are in a good agreement with the observation that intermolecular NOEs were observed only from the phenyl group with the tetrazole ring in losartan and not from any other chemical structures (Figures 5 and 6C). Furthermore, the absence of intermolecular NOEs from the benzylimidazole group and alkyl chain is consistent with the motion of these groups on the GPVI surface during MD simulations.

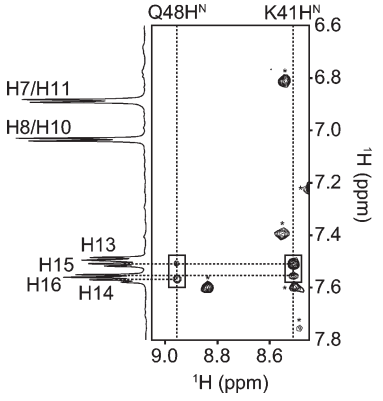

Figure 5. A 1D ^{1}H NMR spectrum of free losartan (left) and an expanded region of the 2D ^{15}N(F2)-edited NOESY spectrum of uniformly ^{2}H,^{15}N-labeled $D1D2^{GPVI}$ upon additional of losartan (right). The box represents intermolecular NOEs between aromatic protons of losartan and amide protons of $D1D2^{GPVI}$. All asterisks are intramolecular NOEs between amide protons in GPVI.

Discussion

Losartan, which was originally considered an AT_1-receptor antagonist, inhibits collagen-stimulated platelet adhesion and aggregation in vitro and in vivo.[9] However, little is known about the target protein of losartan and its inhibitory mechanism for platelet adhesion and aggregation. Collagen-dependent platelet activation is reportedly inhibited via GPVI upon the addition of losartan and **2** according to cellular analyses by using GPVI activating antibodies.[12] In this study, our NMR analyses directly revealed that losartan site-specifically interacts with GPVI, and its binding constant was determined by the CSP experiment (Figure 3). The recognition mechanism between GPVI and collagen has not been experimentally elucidated yet, but Horii et al. presented a GPVI−CRP complex model using docking software and incorporating point mutational analyses.[18−20] The losartan binding site of GPVI determined in this study overlapped the putative CRP binding site, consisting of strands C′ and E of GPVI. If the collagen interaction site is valid, then an inhibitory effect of losartan on collagen-dependent platelet adhesion and aggregation may come about via competitive inhibition with collagen. Recently, we reported that a peptide consisting of 12 amino acids derived by a phage display method directly binds to GPVI and prevents the interaction of GPVI and collagen.[21] This peptide has a competitive inhibitory effect against losartan on the GPVI surface (data not shown). Therefore, the losartan binding site in GPVI would be an attractive site for small molecule inhibition of the GPVI−collagen interaction.

Determining the atomic coordinates of a protein−ligand complex structure with high precision is a critical step in SBDD (structure-based drug discovery). However, structural determination of a protein−ligand complex is still a time-consuming task, requiring, for example, the search for proper soaking and crystallization conditions for a suitable crystal of the complex, since the complex does not necessarily crystallize even if the crystal structure of the target protein alone is available. In such cases, it has been demonstrated that reliable structural models of protein−ligand complexes can be derived by a combination usage of in silico tools and NMR data.[22−25]

In the present study, in order to eliminate program-dependent bias in docking calculations, we used two distinct ligand docking programs. We obtained 17 distinct ligand docking poses by rmsd cluster analysis and further classified them into four groups according to the binding modes of the moiety of losartan on GPVI (Figure 4). Those complex structures that satisfied the intermolecular NOEs between GPVI and losartan are represented in group A, indicating that a key

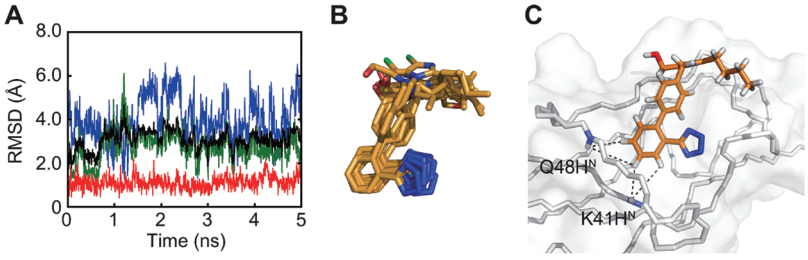

Figure 6. (A) The rmsd values for all atoms of losartan and its functional groups as a function showing a structural drift from initial coordinates in group A during the first 5 ns. Each line is colored as follows: black, all regions; red, phenyl group with tetrazole ring; green, imidazole group; blue, alkyl chain. (B) Superimpositions of the initial GPVI−losartan complex model in group A and the MD simulated 10 structures of every 500 ps. The heavy atoms in the backbones of $D1^{GPVI}$ have been fitted before all protein atoms were stripped. Losartan, which is rendered as a stick model, is colored orange, blue, red, and green for carbon, nitrogen, oxygen, and chloride respectively. (C) Representative docking structure of GPVI (white) and losartan in group A. Observed intermolecular NOEs between GPVI and losartan are represented by a dotted black line.

interaction between the hydrophobic residues in GPVI (Leu38, Leu53, and Tyr66) and the phenyl group in losartan is represented for the losartan binding. Finally, the complex structure was verified by MD simulations with explicit water molecules, and reliable binding poses of losartan could be obtained.

Non-peptide AT_1-receptor antagonists, which reduce blood pressure in human hypertensive subjects, have an additional and separate action in preventing platelet adhesion and aggregation.[9,11,26,27] Among them, it has been revealed that losartan exhibits a GPVI-dependent inhibitory effect on platelet adhesion and aggregation. We have tested the interaction of other AT_1-receptor antagonists, 4′-[[4-methyl-6-(1-methyl-2-benzimidazazolyl)-2-propyl-1-benzimidazolyl]methyl]-2-biphenylcarboxylic acid (telmisartan) and (±)-1-[[(cyclohexyloxy)carbonyl]oxy]ethyl 2-ethyl-1-[[2′-(1*H*-tetrazole-5-yl)[1,1′-biphenyl]-4-yl]methyl]-1*H*-benzimidazole-7-carboxylate (candesartan cilexetil). On the basis of CSP experiments with these ligands, candesartan cilexetil, which has a tetrazole ring, dose-dependently interacts with GPVI but with a lower binding affinity than losartan, while telmisartan, which has carboxylate moiety instead, does not affect the spectrum (data not shown). These results indicate that the tetrazole ring is necessary for the interaction with GPVI, and our MD simulation results definitely support this hypothesis. The phenyl group with the tetrazole ring of non-peptide AT_1-receptor antagonists might be primarily important for the interaction with GPVI, and the key interaction in the GPVI−losartan complex might be not only between the hydrophobic residues in GPVI and the phenyl group in losartan but also between the acidic residues in GPVI (Lys41 and Arg46) and the tetrazole in losartan. Therefore, in order to increase the inhibitory activity for platelet aggregation of losartan, it would be necessary to improve the benzylimidazole group and the alkyl chain moiety.

Conclusion

In this study, we revealed the specific interaction between GPVI and the AT_1-receptor antagonist losartan by using NMR spectroscopy and suggest that this interaction directly inhibits collagen-dependent platelet activation and aggregation. Our approach to construct a protein−ligand complex structure, using a combination of NMR data and in silico tools, has led to a reliable GPVI−losartan complex model in which the losartan binding site was identified as the hydrophobic pocket consisting of strands C′ and E of GPVI. Moreover, the key chemical structure of losartan that interacts with GPVI was specified as the phenyl group with the tetrazole ring, suggesting additional possibilities for improving its activity and specificity as a GPVI antagonist.

Experimental Section

Cloning, Expression, and Purification of the GPVI Ig-like Domain. The nucleotide sequence of the GPVI coding region was prepared from CMK cell cDNA as described in a previous study.[28] Briefly, CMK cells (5×10^5 mL^{-1}) cultured in RPMI 1650 medium with 10% fetal calf serum (Invitrogen) were derived from mature megakaryocytes after 20 nM phorbol 12-myristate 13-acetate (Sigma) treatment. After cells were harvested, the total RNA was isolated by using Trizol (Invitrogen). The cDNA was prepared by reverse transcription with oligo-$(dT)_{12-18}$ primer using Super Script II RT (Invitrogen). The full-length GPVI cDNA was amplified by PCR. The PCR product was ligated to a pCR3.1 vector (Invitrogen) and transformed into *Escherichia coli* strain DH5α. The coding region of the GPVI Ig-like domain ($D1D2^{GPVI}$) was amplified by PCR from full-length GPVI cDNA. The restriction sites *Nde*I and *BamH*I were incorporated into the constructs. Following digestion with *Nde*I and *BamH*I, the pair of PCR products was ligated into pET-15b (Merck). The cloned pET-15b vector was transformed into BL21(DE3) *E. coli* cells.

To generate isotopically labeled proteins for NMR analysis, cells harboring the $D1D2^{GPVI}$ construct were grown in M9 minimal media containing $^{15}NH_4Cl$ and/or [$^{13}C_6$]D-glucose as the sole nitrogen and carbon source, respectively. In the case of the uniformly ^2H,^{13}C,^{15}N-labeled $D1D2^{GPVI}$, cells were grown in M9 media in ^2H_2O (99.5%) containing $^{15}NH_4Cl$ and [$^2H_7$,$^{13}C_6$]D-glucose. Cultures were grown to an OD_{600} of ∼1.8 at 37 °C and then were changed to M9 media (OD_{600} of ∼1.0). IPTG was added to a final concentration of 1 mM to induce expression, and culture growth was continued for 8 h at 37 °C.

Cells were harvested by centrifugation, and the pellets were dissolved in 6 M GdnHCl, 20 mM phosphate (pH 8.0), 500 mM NaCl, and 1 mM DTT. Insoluble debris was removed by centrifugation. His-tagged $D1D2^{GPVI}$ was purified from the supernatant by a HisTrap HP column (GE Healthcare) in denaturing conditions. 2-Mercaptethanol was added to the eluted protein at a final concentration of 10 mM and incubated for 1 h at 37 °C. Reduced $D1D2^{GPVI}$ was diluted 6-fold by 50 mM MES (pH 6.5), 500 mM L-Arg, 250 mM NaCl, 10 mM KCl, 1 mM EDTA, and 0.05% PEG3550 and incubated overnight at 4 °C. The purified protein was then refolded by using multistep dialysis against solutions containing 50 mM MES (pH 6.5), 400 mM L-Arg, 100 mM NaCl, and 1 mM EDTA for a half day. The refolded protein was dialyzed against solutions containing 50 mM MES (pH 6.5), 300 mM glucose, 100 mM NaCl, and 1 mM EDTA for a half day. The refolded $D1D2^{GPVI}$ solution was fractionated over a HiTrap SPHP column (GE Healthcare). After His-tag cleavage of the eluted sample was implemented by thrombin protease, final purification was performed by a HiTrap SPHP column.

The purity of the protein solution was analyzed by SDS−PAGE. Protein concentrations were determined by UV absorbance at 280 nm using molar absorption coefficients (ε) of 1490, 5500, and 125 M^{-1} cm^{-1} for tyrosine, tryptophan, and disulfide bonds, respectively.[29]

Synthesis of CRP and SPR Spectroscopy. All peptides were purchased from BEX Co., Ltd. Cross-linked collagen-related peptide (CRP-XL) was prepared from the backbone peptide $GKO(GPO)_{10}GKOG$ or $GCO(GPO)_{10}GCOG$ as described previously.[13] SPR experiments were performed using a BIAcore 2000 system at 25 °C. Specific binding response data were obtained by subtracting the response obtained using a flow cell that was not coated with ligands. Acid soluble collagen (type I and type III, Chemicon) and CRP were immobilized on a CM5 sensor chip using an amine coupling kit. The binding assay was performed in running buffer HBS-EP (10 mM HEPES, 150 mM NaCl, 3 mM EDTA, 0.005% surfactant P-20, pH 7.4) at a flow rate of 20 μL/min using serial dilutions of $D1D2^{GPVI}$. The data for the construction of the Scatchard plots were obtained from the equilibrium portion of the SPR sensorgrams as described previously.[30]

NMR Data Collection and Assignment of Losartan. Losartan, which was purchased as a powder (Kemprotec Ltd.), was prepared at a final concentration of 15.5 mM in 99.5% ^2H_2O. A final purity of >95% was determined by analytical RPHPLC (Supelcosil ODS column) and UV detection at 227 nm. One-dimensional (1D) ^1H NMR spectra were recorded on a Bruker Avance 700 MHz spectrometer equipped with a 5 mm inverse triple resonance probehead with three-axis gradient coil at 298 K. ^1H NMR spectra were typically recorded with a 10 000 Hz sweep width and 32K data points. The ^1H resonances for losartan were assigned from the two-dimensional (2D) DQF-COSY, TOCSY, and ROESY spectra. The 2D ROESY spectrum was

collected with a mixing time of 200 ms. All NMR spectra were processed using NMRPipe/nmrDraw.[31]

NMR Data Collection of GPVI. NMR experiments were performed in a solvent mixture of 95% H_2O and 5% ^2H_2O in 20 mM HEPES-d_{18} (pH 6.5) and 5% glycerol-d_8 at a final concentration of 0.1−0.3 mM using a Bruker Avance 800 MHz spectrometer equipped with a 5 mm inverse triple resonance probe head with three-axis gradient coil and a cryogenic probe at 298 or 310 K. The 2D $^1H-^{15}N$ TROSY-HSQC, three-dimensional (3D) TROSY-HNCACB, TROSY-HN(CO)CACB, TROSY-HNCA, TROSY-HN(CO)CA, TROSY-HNCO, and TROSY-HN(CA)CO experiments, together with 3D NOESY-TROSY, were performed for backbone assignments. To facilitate the resonance assignment, six samples with 1-^{13}C selective labeling (Pro, Leu, Lys, Arg, Phe, and Tyr) in a ^2H,^{15}N background were prepared and 2D TROSY-HN(CO) experiments were performed to obtain amino acid type information.[17] The proton chemical shift was referenced to the methyl signal of 2,2-dimethyl-2-silapentane-5-sulfonate (DSS) as an external reference at 0 ppm. The ^{13}C and ^{15}N chemical shifts were referenced indirectly to DSS. All NMR spectra were processed using NMRPipe/nmrDraw[31] and analyzed using the software CARA.[32]

For the identification of the losartan recognition site in GPVI, 2D $^1H-^{15}N$ TROSY-HSQC spectra were acquired at a protein concentration of 0.1 mM in the absence or presence of losartan at different molar ratios including 1:0.3, 1:0.6, 1:1, 1:2, 1:4, 1:8, and 1:12 (GPVI:losartan). By superimposition of the HSQC spectra, the shifted cross-peaks of GPVI could be identified and further assigned to the corresponding GPVI residues. The degree of perturbation ($\Delta\delta$) was reflected by an integrated index calculated by the formula $\Delta\delta = [(\Delta\delta_H)^2 + (\Delta\delta_N/5)^2]^{1/2}$, where $\Delta\delta_H$ and $\Delta\delta_N$ denote chemical shift changes of hydrogen and nitrogen, respectively.

For intermolecular NOE measurement between GPVI and losartan, 2D ^{15}N(F2)-edited $^1H-^1H$ NOESY experiments of uniformly ^2H,^{15}N-labeled $D1D2^{GPVI}$ alone and of the bound state in the presence of 8-fold excess losartan were performed with a mixing time of 100 ms at 298 K.

Ligand Docking Simulations. The coordinates of the GPVI N-terminal Ig-like domain (D1, 1−89 aa) used in the docking simulation were obtained from the Protein Data Bank (PDB entry code 2gi7). This crystal structure is registered as a back-to-back dimer form.[18] Each structure model, chains A and B, has some difference in conformation, such as the side chain of Arg46 blocking the losartan binding candidate region in chain B. Therefore, ligand docking simulations were performed against both models of GPVI. Two structures of GPVI were optimized by using the "protein preparation wizard" program (Schrödinger, Inc.). A three-dimensional structure of losartan was created with the LigPrep program (Schrödinger, Inc.) using standard bond lengths and angles.

Ligand docking simulations were based on CSP data and used two different programs: Glide 4.5 (Schrödinger, Inc.) and Sievgene.[33] We used rigid docking and an IFD with the extra precision (XP) mode in the Glide program. IFD simulation was performed by a combination of the docking program Glide and the protein modeling program Prime.[34] The receptor grid was generated within the bounding box so that the center was set to the centroid of the 21 residues from Glu40 to Arg60 in GPVI. In the ligand docking simulation using the Sievgene program, a search for the ligand binding pocket was performed by scanning the entire GPVI surface by using the SiteMap 2.1 program[35] before performing ligand docking because Sievgene does not assign the ligand binding region. The receptor grid was generated with a 6 Å margin to encircle the ligand binding region. Other parameters were set to default for both Glide and Sievgene.

MD Simulations. MD simulations of the protein−ligand complex were performed by using the cosgene program[36] with Amber99 force fields. All models were solvated in a spherical shape with TIP3P (three-site transferable intermolecular potential) water molecules and a distance of 35 Å from the center of mass of the $D1^{GPVI}$−losartan complex structure. A water cap constraint was applied at a distance of 35 Å. All ionizable residues were considered in the standard ionization state at neutral pH. To eliminate residual unfavorable interactions between GPVI and losartan and between the solvent and the complex protein, the whole system was minimized for all atoms until possible bad contacts were removed. After the stability of the model structures was tested via performing 5 ps simulations at a gradient temperature of 0−300 K, simulations were performed for 5 ns at a constant temperature of 300 K. During the simulations, the time step for integrating the Newton equations was 2 fs with a SHAKE constraint[37] on all bonds containing hydrogen atoms, and the nonbonded cutoff was 12 Å. Structures were saved every 2 ps. The representative GPVI−losartan complex structure was obtained from a minimization of the average structure of 600 complex models that appeared to be stabilizing during MD simulation (1−4 ns).

Acknowledgment. This work was supported by the New Energy and Industrial Technology Development Organization (NEDO).

Supporting Information Available: Breakdown list of the clustering analysis for protein−ligand docking simulation; figure showing each structure of losartan presented in Figure 6B. This material is available free of charge via the Internet at http://pubs.acs.org.

References

(1) Ruggeri, Z. M. Platelets in atherothrombosis. *Nat. Med.* **2002**, *8*, 1227–1234.
(2) Nieswandt, B.; Watson, S. P. Platelet−collagen interaction: Is GPVI the central receptor? *Blood* **2003**, *102*, 449–461.
(3) Farndale, R. W.; Sixma, J. J.; Barnes, M. J.; De Groot, P. G. The role of collagen in thrombosis and hemostasis. *J. Thromb. Haemostasis* **2004**, *2*, 561–573.
(4) Nieswandt, B.; Brakebusch, C.; Bergmeier, W.; Schulte, V.; Bouvard, D.; Mokhtari-Nejad, R.; Lindhout, T.; Heemskerk, J. W.; Zirngibl, H.; Fassler, R. Glycoprotein VI but not $\alpha2\beta1$ integrin is essential for platelet interaction with collagen. *EMBO J.* **2001**, *20*, 2120–2130.
(5) Qian, M. D.; Villeval, J.-L.; Xiong, X.; Jandrot-Perrus, M.; Nagashima, K.; Tonra, J.; McDonald, K.; Goodearl, A.; Gill, D. Anti GPVI human antibodies neutralizing collagen-induced platelet aggregation isolated from a combinatorial phage display library. *Hum. Antibodies* **2002**, *11*, 97–105.
(6) Massberg, S.; Konrad, I.; Bultmann, A.; Schulz, C.; Munch, G.; Peluso, M.; Lorenz, M.; Schneider, S.; Besta, F.; Muller, I.; Hu, B.; Langer, H.; Kremmer, E.; Rudelius, M.; Heinzmann, U.; Ungerer, M.; Gawaz, M. Soluble glycoprotein VI dimer inhibits platelet adhesion and aggregation to the injured vessel wall in vivo. *FASEB J.* **2004**, *18*, 397–399.
(7) Krämer, C.; Sunkomat, J.; Witte, J.; Luchtefeld, M.; Walden, M.; Schmidt, B.; Tsikas, D.; Böger, R. H.; Forssmann, W. G.; Drexler, H.; Schieffer, B. Angiotensin II receptor-independent antiinflammatory and antiaggregatory properties of losartan: role of the active metabolite EXP3179. *Circ. Res.* **2002**, *90*, 770–779.
(8) Schmidt, B.; Schieffer, B. Angiotensin II AT1 receptor antagonists. Clinical implications of active metabolites. *J. Med. Chem.* **2003**, *46*, 2261–2270.
(9) Kalinowski, L.; Matys, T.; Chabielska, E.; Buczko, W.; Malinski, T. Angiotensin II AT1 receptor antagonists inhibit platelet adhesion and aggregation by nitric oxide release. *Hypertension* **2002**, *40*, 521–527.
(10) Wang, G. R.; Zhu, Y.; Halushka, P. V.; Lincoln, T. M.; Mendelsohn, M. E. Mechanism of platelet inhibition by nitric oxide: in vivo phosphorylation of thromboxane receptor by cyclic GMP-dependent protein kinase. *Proc. Natl. Acad. Sci. U.S.A.* **1998**, *95*, 4888–4893.
(11) Montón, M.; Jiménez, A.; Núñez, A.; López-Blaya, A.; Farré, J.; Gómez, J.; Zalba, L. R.; Sánchez de Miduel, L.; Casado, S.; López-Farré, A. Comparative effects of angiotensin II AT1-type receptor

antagonists in vitro on human platelet activation. *J. Cardiovasc. Pharmacol.* **2000**, *35*, 906–913.
(12) Grothusen, C.; Umbreen, S.; Konrad, I.; Stellos, K.; Schulz, C.; Schmidt, B.; Kremmer, E.; Teebken, O.; Massberg, S.; Luchtefeld, M.; Schieffer, B.; Gawaz, M. EXP3179 inhibits collagen-dependent platelet activation via glycoprotein receptor-VI independent of AT_1-receptor antagonism. *Arterioscler., Thromb., Vasc. Biol.* **2007**, *27*, 1184–1190.
(13) Mortón, L. F.; Hargreaves, P. G.; Farndale, R. W.; Young, R. D.; Barnes, M. J. Integrin $\alpha 2\beta 1$-independent activation of platelets by simple collagen-like peptides: collagen tertiary (triple-helical) and quaternary (polymeric) structures are sufficient alone for $\alpha 2\beta 1$-independent platelet reactivity. *Biochem. J.* **1995**, *306*, 337–344.
(14) Kehrel, B.; Wierwille, S.; Clemetson, K. J.; Anders, O.; Steiner, M.; Knight, C. G.; Farndale, R. W.; Okuma, M.; Barnes, M. J. Glycoprotein VI is a major collagen receptor for platelet activation: It recognizes the platelet-activating quaternary structure of collagen, whereas CD36, glycoprotein IIb/IIIa, and von Willebrand factor do not. *Blood* **1998**, *91*, 491–499.
(15) Knight, C. G.; Morton, L. F.; Onley, D. J.; Peachey, A. R.; Ichinohe, T.; Okuma, M.; Farndale, R. W.; Barnes, M. J. Collagen-platelet interaction: Gly-Pro-Hyp is uniquely specific for platelet Gp VI and mediates platelet activation by collagen. *Cardiovasc. Res.* **1999**, *41*, 450–457.
(16) Miura, Y.; Takahashi, T.; Jung, S. M.; Moroi, M. Analysis of the interaction of platelet collagen receptor glycoprotein VI (GPVI) with collagen. *J. Biol. Chem.* **2002**, *277*, 46197–46204.
(17) Takeuchi, K.; Ng, E.; Malia, T. J.; Wagner, G. 1-^{13}C amino acid selective labeling in a $^{2}H^{15}N$ background for NMR studies of large proteins. *J. Biomol. NMR* **2007**, *38*, 89–98.
(18) Horii, K.; Kahn, M. K.; Herr, A. B. Structural basis for platelet collagen responses by the immune-type receptor glycoprotein VI. *Blood* **2006**, *108*, 936–942.
(19) Smethurst, P. A.; Joutsi-Korhonen, L.; O'Conner, M. N.; Wilson, E.; Jenning, N. S.; Gamer, S. F.; Zhang, Y.; Knight, C. G.; Dafforn, T. R.; Buckle, A.; IJsseldijk, M. J. W.; de Groot, P. G.; Watkins, N. A.; Farndale, R. W.; Ouwehand, W. H. Identification of the primary collagen-binding surface on human glycoprotein VI by site-directed mutagenesis and by a blocking phage antibody. *Blood* **2004**, *103*, 903–911.
(20) O'Conner, M. N.; Smethurst, P. A.; Farndale, R. W.; Ouwehand, W. H. Gain- and loss-of-function mutants confirm the importance of apical residues to the primary interaction of human glycoprotein VI with collagen. *J. Thromb. Haemostasis* **2006**, *4*, 869–873.
(21) Kato-Takagaki, K.; Mizukoshi, Y.; Yoshizawa, Y.; Akazawa, D.; Torii, Y.; Ono, K.; Tanimura, Y.; Shimada, I.; Takahashi, H. Structural and interaction analysis of glycoprotein VI-binding peptide selected from phage display library. *J. Biol. Chem.* **2009**, *284*, 10720–10727.
(22) Bertini, I.; Fragai, M.; Giachetti, A.; Luchinat, C.; Maletta, M.; Parigi, G.; Yen, K. J. Combining in silico tools and NMR data to validate protein−ligand structural models: application to matrix metalloproteinases. *J. Med. Chem.* **2005**, *48*, 7544–7559.
(23) Schieborr, U.; Vogtherr, H.; Elshorst, B.; Betz, M.; Grimme, S.; Pescatore, B.; Langer, T.; Saxena, K.; Schwalbe, H. How much NMR data is required to determine a protein−ligand complex structure? *ChemBioChem* **2005**, *6*, 1891–1898.
(24) Constantine, K. L. Evaluation of site-directed spin labeling for characterizing protein−ligand complexes using simulated restraints. *Biophys. J.* **2001**, *81*, 1275–1284.
(25) Stark, J.; Powers, R. Rapid protein−ligand costructures using chemical shift perturbations. *J. Am. Chem. Soc.* **2008**, *130*, 535–545.
(26) Chabielska, E.; Pawlak, R.; Golatowski, J.; Rółkowski, R.; Pawlak, D.; Buczko, W. Losartan inhibits experimental venous thrombosis in spontaneously hypertensive rats. *Thromb. Res.* **1998**, *90*, 271–278.
(27) Müller, D. N.; Mervaala, E. M. A.; Dechend, R.; Fiebeler, A.; Park, J.-K.; Schmidt, F.; Theuer, J.; Breu, V.; Mackman, N.; Luther, T.; Schneider, W.; Gulba, D.; Ganten, D.; Haller, H.; Luft, F. C. Angiotensin II (AT_1) receptor blockade reduces vascular tissue factor in angiotensin II-induced cardiac vasculopathy. *Am. J. Pathol.* **2000**, *157*, 111–122.
(28) Ezumi, Y.; Uchiyama, T.; Takayama, H. Molecular cloning, genomic structure, chromosomal localization, and alternative splice forms of the platelet collagen receptor glycoprotein VI. *Biochem. Biophys. Res. Commun.* **2000**, *277*, 27–36.
(29) Pace, C. N.; Vajdos, F.; Lee, L.; Grimsley, G.; Gray, T. How to measure and predict the molar absorption coefficient of a protein. *Protein Sci.* **1995**, *4*, 2411–2423.
(30) Rich, R. L.; Kreikemeyer, B.; Owens, R. T.; LaBrenz, S.; Narayana, S. V. L.; Weinstock, G. M.; Murray, B. E.; Hook, M. Ace is a collagen-binding MSCRAMM from *Enterococcus faecalis*. *J. Biol. Chem.* **1999**, *274*, 26939–26945.
(31) Delaglio, F.; Grzesiek, S.; Vuister, G. W.; Zhu, G.; Pfeifer, J.; Bax, A. NMR Pipe: a multidimensional spectral processing system based on UNIX pipes. *J. Biomol. NMR* **1995**, *6*, 277–293.
(32) Keller, R.; Wüthrich, K. Computer-Aided Resonance Assignment (CARA). http://www.nmr.ch.
(33) Fukunishi, Y.; Mikami, Y.; Nakamura, H. Similarities among receptor pockets and among compounds: analysis and application to in silico ligand screening. *J. Mol. Graphics Modell.* **2005**, *24*, 34–45.
(34) Sherman, W.; Day, T.; Jacobson, M. P.; Friesner, R. A.; Farid, R. Novel procedure for modeling ligand/receptor induced fit effects. *J. Med. Chem.* **2006**, *49*, 534–553.
(35) Halgren, T. New method for fast and accurate binding-site identification and analysis. *Chem. Biol. Drug Des.* **2007**, *69*, 146–148.
(36) Kim, J. G.; Fukunishi, Y.; Nakamura, H. Multicanonical molecular dynamics algorithm employing adaptive force-biased iteration scheme. *Phys. Rev. E* **2004**, 057103.
(37) Ryckaert, J. P.; Ciccotti, C.; Berendsen, H. J. C. Numerical integration of the Cartesian equations of motion of a system with constraints: molecular. *J. Comput. Phys.* **1977**, *23*, 327–341.
(38) Goddard, T. D.; Kneller, D. G. *SPARKY*, version 3; University of California: San Francisco, CA, 2005.